Preprints of the 2012 20th Mediterranean Conference on Control & Automation (MED), Barcelona, Spain, July 3-6, 2012



# Robust LMI Control of a Buck-Boost Converter with Low Ripple Propagation

J.V. Inglés, P. Garcés, R. Leyva
Dept. of Electronic, Electrical and Automatic Control Engineering
Universitat Rovira i Virgili
Tarragona, Spain

***Abstract*—This paper proposes a new robust control strategy to prevent the current ripple propagation into the dc-dc converter input, thus avoiding converter malfunctions. Concretely, we apply the new strategy to a buck-boost converter. The strategy is based on LMI control and use readily, fast convex optimization algorithms to obtain the solution. The control objective is maximizing the current disturbance rejection, where current ripple propagation and usual, prescribed dynamic performances are ensured. The paper describes the control design procedure, besides an illustrative example and simulation verifications. Simulation waveforms are in perfect agreement with objective function and performances constraints of the control design. That is, the current ripple propagation is almost zero and other prescribed constraints are satisfied.**

## I. Introduction

SWITCHING converters are efficient power processing systems that adapt and regulate the output voltage to load requirements. In this paper, we analyze the buck-boost converter. This dc-dc switching topology is able to step up or step down the voltage of the primary source. Power Electronics engineers add feedback loops to improve converter dynamical performances. State variable signals of these systems are contaminated with ripple noise. When ripple noise is propagated into the control signal, which corresponds to the MOSFET duty cycle, performances are degraded. Thus, a control design based on an average model of the converter may fail to work properly when it is implemented. These systems are nonlinear and have uncertain parameters. This is the reason that has prompted several authors to propose nonlinear and robust controller designs. Some of the first works on nonlinear control for power converters can be found in [1], [2], where the author proposes strategies based on quadratic Lyapunov functions. More recently, Cortes et al. [3], He and Luo [4] and Leyva et al. [5], derive robust nonlinear controllers for these Power Electronics plants

This work was supported in part by the Spanish Ministerio de Educación y Ciencia DPI 2010-1648.

J. V. Inglés and R. Leyva are with the Departament d'Enginyeria Electrònica, Elèctrica I Automàtica, Escola Tècnica Superior d'Enginyeria, Universitat Rovira i Virgili, 43007 Tarragona, Spain (e-mail: ramon.leyva@urv.cat).

In the paper, we propose a new control design based on linear matrix inequalities (LMI). LMI control techniques have been extensively developed during the last two decades. The reason is that this approach allows us to impose a great number of dynamical constraints, unlike classical techniques. LMI control uses convex optimization algorithms to obtain the controller parameters [6], [7]. LMI control consists of modeling the controller design process as a convex optimization program that can be readily solved by standard interior-point methods. Using this procedure ensures that either the optimum is rapidly achieved or the infeasibility is promptly detected.

LMI technique has been applied in dc-dc converters domain as references [8], [9] state. These references propose controller designs that ensure stability, a prescribed close-loop pole placement, and limit the control effort but do not take into account switching ripple propagation. Unlike the previous works, we propose a novel LMI constraint to ensure that the control signal is almost ripple-free. Thus, the novel control strategy for buck-boost converters, that we propose here, limits the switching noise propagation whereas optimize the current load rejection, satisfying the usual robustness and dynamical constraints. The paper describes the control strategy and shows simulation results that corroborate the approach.

The paper is organized as follows: in section II, we describe the buck-boost converter dynamics taking into account the uncertain parameter and disturbance signals. LMI design expressions are explained in section III. Controller values and simulation verifications are reported in section IV. Finally, we summarize the main ideas in section V.

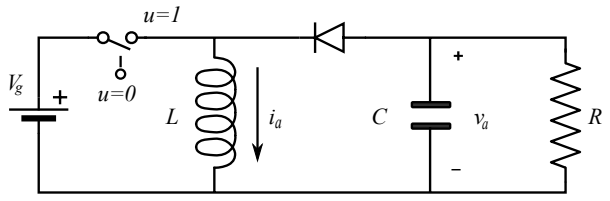


Figure 1. Buck-boost converter.

978-1-4673-2529-5/12/$31.00 ©2012 IEEE

## II. STATE-SPACE MODEL

In this section, we review the buck-boost converter dynamics and complement the model with two additional state variables; the first of them stands for the integral error of the output voltage, and the second additional state variable is used to obtain a filtered signal of the duty-cycle that permit us to constrain the ripple propagation. Moreover, we consider the uncertain parameters of the converter by means of a polytopic model.

### *A. Augmented model of the buck-boost converter*

Fig. 1 shows a buck-boost converter whose dynamic behavior during $T_{ON}$ *(u = 1)* and $T_{OFF}$ *(u = 0)* can be expressed as follows

$$\dot{x}_a = (A_{ON}x_a + B_{ON})u + (A_{OFF}x_a + B_{OFF})(1-u) \quad (1)$$

where

$$A_{ON} = \begin{bmatrix} 0 & 0 \\ 0 & -\frac{1}{RC} \end{bmatrix}, \quad A_{OFF} = \begin{bmatrix} 0 & \frac{1}{L} \\ -\frac{1}{C} & -\frac{1}{RC} \end{bmatrix}$$

$$B_{ON} = \begin{bmatrix} \frac{V_g}{L} \\ 0 \end{bmatrix}, B_{OFF} = \begin{bmatrix} 0 \\ 0 \end{bmatrix}$$

and

$$x_a^T = \begin{bmatrix} i_a & v_a \end{bmatrix}$$

The state vector components are $i_a$, which represents the inductor current, and $v_a$, which represents the capacitor voltage. These variables are measurable and available for feedback purposes. Parameters $R$, $L$ and $C$ stand for the values of resistor, inductor and capacitor, respectively. $V_g$ represents the feed-voltage.

Considering that the system variables consist of two components

$$\begin{aligned} x_a &= X + x \\ d_a &= D + d \end{aligned} \quad (2)$$

where $x$ and $d$ are the incremental values of the state vector and duty-cycle and $X$ and $D$ are the equilibrium values, that corresponds to,

$$X = \begin{bmatrix} \frac{V_g D}{RD'^2} \\ -\frac{V_g D}{D'} \end{bmatrix}, \text{ and } x = \begin{bmatrix} i \\ v \end{bmatrix} \text{ where } D' = 1 - D \quad (3)$$

$i$ and $v$ stands for the values of current and voltage around the equilibrium.

Hence, equation (1) can be rewritten as

$$\dot{x} = \bar{A}x + \bar{B}d \quad (4)$$

where

$$\bar{A} = \begin{bmatrix} 0 & \frac{D'}{L} \\ -\frac{D'}{C} & -\frac{1}{RC} \end{bmatrix}, \quad \bar{B} = \begin{bmatrix} \frac{V_g D}{LD'} \\ \frac{V_g D}{CRD'^2} \end{bmatrix}$$

Fig. 2 is a circuital model of expression (4), where two disturbance signals, modeled as current sources, have been added. The first one, named $i_r$ , models the current ripple and the second one, named $i_l$ , takes into account the load disturbances.

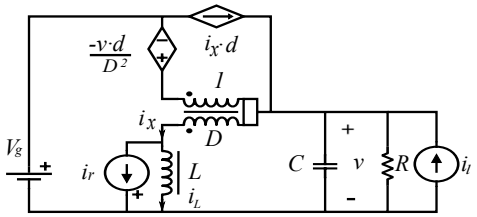


Figure 2. Buck-boost small signal with disturbance signals.

Considering the disturbance sources the expression (4) is modified as,

$$\dot{x} = \bar{A}x + \bar{B}d + \bar{B}_l i_l + \bar{B}_r i_r \quad (5)$$

where input vector associated to each disturbance signals is,

$$\bar{B}_l = \begin{bmatrix} 0 \\ -\frac{1}{C} \end{bmatrix} \text{ and } \bar{B}_r = \begin{bmatrix} 0 \\ \frac{D'}{C} \end{bmatrix}$$

The state variable $x_3$ is the integral of the error signal obtained from the difference between $V_{ref}$ and the output voltage $v_a$. That is,

$$\dot{x}_3 = V_{ref} - v_a \quad (6)$$

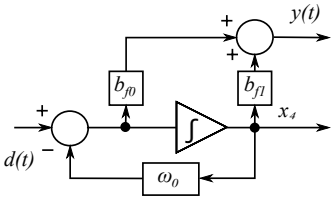


Figure 3. High-pass filter of the duty-cycle signal.

$x_4$ is the variable expression of a filter whose input is the duty cycle *d(t)* and the output is *y(t)*. Namely,

$$\dot{x}_4 = d - \omega_0 x_4 \quad (7)$$

$$y = b_{f1}x_4 + b_{f0}d \quad (8)$$

The following expression shows the state-space averaged and linearized model of the buck-boost converter.

$$\begin{cases} \dot{x}(t) = Ax(t) + B\,d(t) + B_l i_l(t) + B_r i_r(t) \\ z(t) = C_z x(t) + D_{zd}\,d(t) + D_{zl}\,i_l(t) \\ y(t) = C_y x(t) + D_{yd}\,d(t) + D_{yr}\,i_r(t) \end{cases} \quad (9)$$

being the augmented state vector,

$$x^T = \begin{bmatrix} i & v & x_3 & x_4 \end{bmatrix}$$

The matrices of the state-space representation are as follows.

$$A=\begin{pmatrix} 0 & \frac{D'}{L} & 0 & 0 \\ \frac{-D'}{C} & \frac{-1}{CR} & 0 & 0 \\ 0 & -1 & 0 & 0 \\ 0 & 0 & 0 & -\omega_0 \end{pmatrix}, B_u=\begin{pmatrix} \frac{V_g D}{D'L} \\ \frac{V_g D}{CRD'^2} \\ 0 \\ 1 \end{pmatrix}$$

$$B_l=\begin{pmatrix} 0 \\ \frac{1}{C} \\ 0 \\ 0 \end{pmatrix}, B_r=\begin{pmatrix} 0 \\ \frac{-D'}{C} \\ 0 \\ 0 \end{pmatrix} \quad (10)$$

Therefore, the output $z$ corresponds to the state variable $v$, which represents the controlled output. The output $y$ (see Fig. 3) corresponds to the filter output and both have to fulfill the prescribed control requirements. The remaining state-space matrices are:

$$C_z = [\,0\ 1\ 0\ 0\,],\ D_{zl}=[0],\ D_{zd}=[0]$$
$$C_y = [\,0\ 0\ 0\ b_{f1}\,],\ D_{yr}=[0],\ D_{yd}=[b_{f2}]$$

*B. A polytopic model of uncertain converter dynamics*

In this subsection, we propose a polytopic representation of the uncertainty compatible with the LMI description. Since the model matrices do not depend, a priori, linearly on these parameters, we define the following uncertain parameter

$$\begin{aligned} D' &\in [\ D'_{\min}\quad D'_{\max}\ ] \\ \beta &\in [\ \frac{1}{R_{\max}}\quad \frac{1}{R_{\min}}\ ] \\ \delta &\in \left[\ \frac{D_{\min}}{D'_{\max}}\quad \frac{D_{\max}}{D'_{\min}}\ \right] \\ \varepsilon &\in \left[\ \frac{D_{\min}}{R_{\max}D'^2_{\max}}\quad \frac{D_{\max}}{R_{\min}D'^2_{\min}}\ \right] \end{aligned} \quad (11)$$

These parameters can be grouped in a vector $p=\left[\ D'\ \ \frac{1}{R}\ \ \frac{D}{D'}\ \ \frac{D}{RD'^2}\ \right]$. Admissible values of parameters vector $p$ are inside a polytope of dimension 4; namely, an hiperectangle with 16 vertices $\{v_1,\ldots,v_{16}\}$. We can express this issue as $p$ belongs a convex combination of vertices of the uncertain parameter space, namely,

$$p=\sum_1^{16}\alpha_i v_i \ \text{ such that } \ \alpha_i>0 \ \text{ and } \ \sum_1^{16}\alpha_i=1 \quad (12)$$

Uncertain converter parameters are $R$ and $D$. Nevertheless the fact of including some additional uncertain parameters such as $\delta$ and $\varepsilon$ implies preservation of convexity. Convex domains easy the optimization procedures used in robust control design technique. However, the solution is potentially conservative. Since the system matrices depend linearly on parameters vector $p$, we can map the parameter polytope to a polytope of system matrices whose vertices $\{\Gamma_1,\ldots,\Gamma_{16}\}$ are the images of the vertices of the parameter polytope $\{v_1,\ldots,v_{16}\}$. Namely,

$$\left[A(p),\quad B(p),\quad B_r(p)\right]=\sum_1^{16}\alpha_i\Gamma_i$$

$$\text{such that} \qquad \alpha_i>0 \ \text{ and } \ \sum_1^{16}\alpha_i=1 \quad (13)$$

where $\Gamma_i=\left[\ A(v_i),\quad B(v_i),\quad B_r(v_i)\ \right]$

Based on the uncertainty model described above, the synthesis objective is finding a state-feedback gain $F$; that is $d = Fx$, that ensure a maximum level of load disturbance rejection ensuring, and simultaneously, a smooth enough control signal, while close-loop poles are inside a prescribed area and the control effort is bounded. In next section, we will establish the LMI conditions which express these design requirements.

## III. LMI DESIGN SPECIFICATION

This section introduces the concept LMI and presents the constraints used in the controller synthesis.

*A. Stability as LMI constraint*

We can ensure stability for a dynamical system by finding a Lyapunov function $V$ such that it is positive definite and its derivative with respect to time $dV/dt$ is negative definite.

Therefore, given the following autonomous linear system,

$$\dot{x}=Ax \quad (14)$$

Stability demonstration involves finding a matrix $P$ of adequate dimension such that satisfy

$$\exists P>0 \quad s.t. \quad A'P+PA<0 \quad (15)$$

where the sign > stands for positive definite and < for negative definite. Conditions (15) are linear matrix inequalities of $P$. Thus finding $P$ such that satisfies (15) can be cast as a feasibility problem in convex optimization [6].

Similarly, we can consider the next system

$$\dot{x}=Ax+Bd \quad (16)$$

with the linear state feedback control $d = F x$ .

Then the system (16) with feedback $d = F x$ is stable if there exits $P$ and $F$, of adequate dimensions, such that fulfill the following condition

$$(A+BF)^T P+P(A+BF)<0 \quad (17)$$

Condition (17) can be rewritten by means of a congruence transformation [6] as

$$\begin{cases} W>0 \\ AW+WA^T+BY+Y^TB^T<0 \end{cases} \quad (18)$$

where $W=P^{-1}$ and $Y=FW$ , or equivalently $F=YW^{-1}$

Hence, we can obtain all the feedback gain vectors $F$ that stabilize the system (16) by finding all $W$ and $Y$ that fulfill (18).

*B. LMI design constraints*

We analyze the $H_\infty$ performance, the pole placement and the control effort as requirements that should be imposed in the controller design.

*1) $H_\infty$ Control Design LMI*

We consider that the feedback controlled system (9) with a linear feedback ***d(t)*** = ***Fx(t)*** is affected by the disturbance signal $i_l$ and the disturbance signal $i_r$ ; that is,

$$\begin{cases} \dot{x}(t) = (A + BF)x(t) + B_l i_l(t) + B_r i_r(t) \\ z(t) = (C_z + D_{zd}F)x(t) + D_{zl} i_l(t) \\ y(t) = (C_y + D_{yd}F)x(t) + D_{yr} i_r(t) \end{cases} \quad (19)$$

We desire to impose restrictions on the controller gain vector $F$ such that the energy gain of the output $z(t)$ is not larger than a certain value $\gamma_l$, that is

$$\|z\|_2 < \gamma_l \|i_l\|_2 \qquad \forall i_l \in L_2 \quad (20)$$

In addition, we impose, next constraint to prevent the ripple propagation

$$\|y\|_2 < \gamma_r \|i_r\|_2 \qquad \forall i_r \in L_2 \quad (21)$$

This means that at any frequency of the disturbance signals will not be amplified more that $\gamma_l$ or $\gamma_r$, respectively. The preceding constraints (20)-(21) can be expressed equivalently by means of the following LMIs,

$$\begin{bmatrix} AW + WA^T + BY + Y^T B^T & B_l & WC_z^T + Y^T D_{zu}^T \\ B_l^T & -\gamma_l I & 0 \\ C_z W + D_{zu} Y & 0 & -\gamma_l I \end{bmatrix} < 0 \quad (22)$$

and

$$\begin{bmatrix} AW + WA^T + BY + Y^T B^T & B_r & WC^T{}_y + Y^T D^T{}_{yu} \\ B^T{}_r & -\gamma_r I & 0 \\ C_y W + D_{yu} Y & 0 & -\gamma_r I \end{bmatrix} < 0 \quad (23)$$

where $W=P^{-1}$ and $Y=FW$.

This result can be readily extended to uncertain systems with a polytopic representation [10].

*2) LMI Formulation for pole-placement*

Another important constraint to be imposed to a family of systems dynamics is the pole placement. We desire that the closed-loop poles are inside a prescribed region. This region ensures a minimum decay rate **α**, a minimum damping ratio **ζ** and a maximum natural frequency ***ω=r***. Thus, this region bounds the maximum overshoot, the rising time and the settling time.

The constraint of decay rate is imposed by means of the following LMI,

$$AW + WA^T + BY + Y^T B^T + 2\alpha W < 0 \quad (24)$$

The damping ratio is limited by the following LMI,

$$\begin{bmatrix} \cos\theta(AW + WA^T + BY + Y^T B^T) & \\ \sin\theta(-AW + WA^T - BY + Y^T B^T) & \\ \sin\theta(AW - WA^T + BY - Y^T B^T) & \\ \cos\theta(AW + WA^T + BY + Y^T B^T) & \end{bmatrix} < 0 \quad (25)$$

In addition, bounds on the natural frequency involve the following LMI

$$\begin{bmatrix} -rW & WA^T + Y^T B^T \\ AW + BY & -rW \end{bmatrix} < 0 \quad (26)$$

A detailed explanation about the previous LMIs and their extension to a family of systems can be found in [11].

*3) LMI constraint on control input*

A control that fulfills with all the previous restrictions but that involve an excessive gain $F$ would saturate the duty cycle, and would worsen the performances. Thus, we bound the control effort $||d(t)|| \le \mu$, along the trajectory for any initial condition $x(0)$ inside the ellipsoid $x(0)^T W^{-1} x(0) \le 1$ by means of the following two additional LMIs

$$\begin{bmatrix} 1 & x(0)^T \\ x(0) & W \end{bmatrix} \ge 0, \quad \begin{bmatrix} W & Y^T \\ Y & \mu^2 I \end{bmatrix} \ge 0 \quad (27)$$

where again $W = P^{-1}$ and $Y=FW$.

The previous design LMI allows us to obtain robust, efficient control laws, in next section where we instantiate the parameters that correspond to the experimental prototype.

## IV. CONTROL DESIGN AND SIMULATION RESULTS

In this section, we describe the LMI control procedure applied to buck-boost converter model (9) taking into account the corresponding polytopic uncertainties (11).

The parameters of the dc-dc converter can be found in Table I.

TABLE I.
BUCK-BOOST CONVERTER PARAMETERS

| ***Parameter*** | ***Value*** |
|---|---|
| *R* | *[10, 50] Ω* |
| *D'* | *0,5* |
| *v, $V_{ref}$* | *-12 V* |
| *C* | *100 μF* |
| *L* | *100 μH* |
| *$T_s$* | *10 μs* |

The values of pole placement can be found in table II.

*A. Controller optimization problem*

The procedure consists of finding the feedback gain $F$ such that the current disturbance rejection is maximized; that is, the minimizing sum of parameters $\gamma_l+\gamma_r$ of LMI (22),(23). As long as, the minimization is subjected to constraints on stability, which corresponds to LMI (24), on pole placement (25)-(26), and on control effort LMIs (27), for each vertex of the polytopic representation of the model. Thus, the control

design procedure can be expressed by means of the following optimization program.

$$\min_{W,Y}(\gamma_l + \gamma_r)$$

$$\text{subject to (24)-(27)} \quad \forall\{\Gamma_i\}, \quad i = \{1,\ldots,16\} \tag{28}$$

Given the control parameters of table I, we obtain the optimal feedback gain vector that corresponds to

$$F = \begin{bmatrix} -0.016 & 0.006 & -6.4 & 5.7e+5 \end{bmatrix} \tag{29}$$

The guaranteed H∞ bounds from disturbances to the considered outputs are $\gamma_l = 10.47$ and $\gamma_r = 0.79$, which corresponds to *20.4* dB and -2.05 *dB*, respectively.

TABLE II.
POLE PLACEMENT PARAMETERS

| *Parameter* | *Value* |
|---|---|
| α | 130 |
| r | $2\pi / 10T_s$ |
| ζ | 0.9 |

*B. MATLAB simulation result*

In this section, we show the dynamic behavior of proposed control corresponding to optimization program (28) where the ripple propagation is optimized.

In order to illustrate the proposed control design, we compare it with a common one that does not add the filter state variable x4 and optimize only the current disturbance rejection $\gamma_l$. The common one can be expressed by the following optimization program,

$$\min_{W,Y}(\gamma_l)$$

$$\text{subject to (24)-(27)} \tag{30}$$

The common LMI control has 3 state variables, thus the feedback gain vector has 3 components. Since we do not take into account any bound on $\gamma_r$, we can expect a better optimal value of parameter $\gamma_l$.

Considering the same parameters of table I and II, the optimal gain vector *F* corresponds to,

$$F=[0.9, -0.58, 367] \tag{31}$$

And the optimal load disturbance rejection is $\gamma_l = 5.6$, which corresponds to *14.95* dB, that is slightly better than in the low ripple propagation program (28).

The switched model of Fig. 1 with the controller *F* has been implemented using MATLAB Simulink. Fig. 4 shows the buck-boost converter schema in MATLAB.

Fig. 5a depicts the output voltage waveform when the controller operates at the nominal equilibrium point and a load step change of 1 A appears for both controllers. It can be noted that the voltage output response presents a time constant of approximately *10 ms*, that corresponds to a decay rate of 400, which larger than the minimum guaranteed decay rate (*α=130*). Furthermore, the output voltage exhibits a damped overshoot that agrees with the damping ratio restriction. Inductor current transient is depicted in Fig. 5b for both controllers. Control signal *d* corresponding to program (28), is represented in Fig. 6a. The same signal is depicted in Fig 6b for the common controller without filter corresponding to program (30). Fig. 7 shows both duty cycles in the same scale, where it can be appreciated that the ripple propagation is *34dB* smaller in our proposed approach.

It can be noted, that performance values are very similar in both approaches, however the proposed robust control overcomes the duty cycle propagation drawbacks.

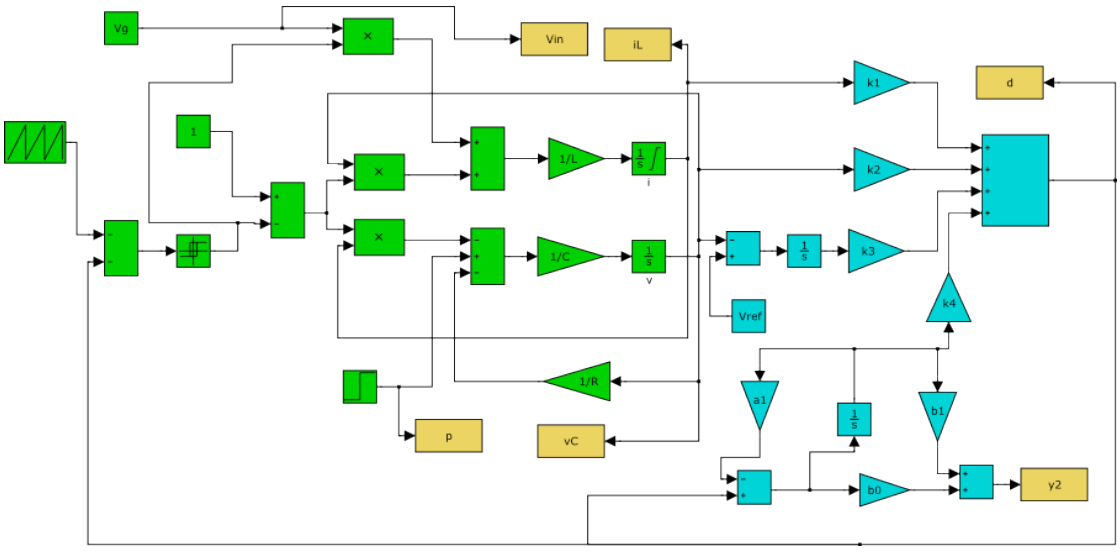

Figure 4 MATLAB-Simulink schematic of the proposed LMI controlled buck-boost converter.

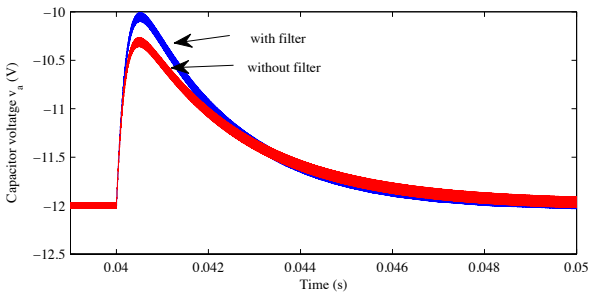


(a)

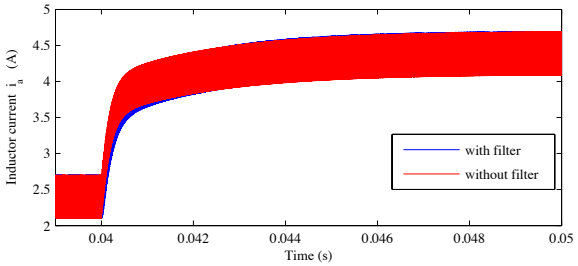


(b)

Figure 5. Simulated transient response for a loading step of 1 A. a) Capacitor voltage. b) Inductor current.

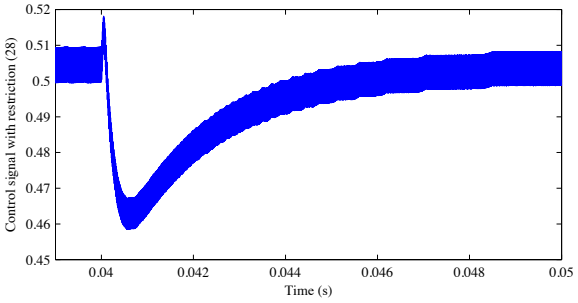


(a)

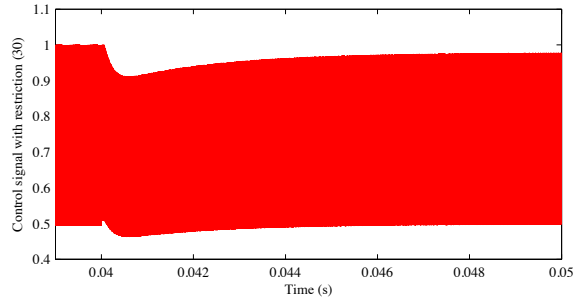


(b)

Figure 6. Transient duty cycle *d* for a loading step of 1 A. a) for LMI program (28). b) for LMI program (30).

## V. Conclusions

This paper proposed a robust control design based on LMI for switching converter that maximizes the load disturbance rejection, as long as, prevents from ripple propagation. In addition, the control ensures stability, performances associates to pole placement and a maximum control effort.

This method has been applied to a buck-boost converter and we have compared the results with a common LMI design that do not constrain the ripple propagation.

Simulation verification corroborates that the proposed control provides almost the same performances without ripple propagation drawbacks.

Proposals to extent the method to other converters have been studied.

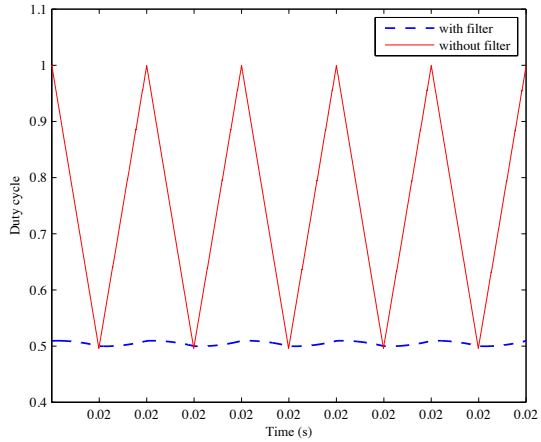


Figure 7. Detail of the duty cycle signal. Dotted line corresponding to the proposed LMI approach (28). Solid line according to LMI program (30).

## References


[1] Sanders S.R., Verghese G.C.: 'Lyapunov-based control for switched power converters', IEEE Trans. Power Electron. 1992, 7, (1), pp. 17–24

[2] Kawasaki N., Nomura H., Masuhiro M.: 'A new control law of bilinear DC-DC converters developed by direct application of Lyapunov', IEEE Trans. Power Electron., 1995, 10, (3), pp. 318–325

[3] Cortes D., Alvarez J., Fradkov A.: 'Tracking control of the boost converter', IEE Proc. Control Theory Appl., 2004, 151, (2), pp. 218–224

[4] He Y., Luo F.L.: 'Sliding-mode control for dc –dc converters with constant switching frequency', IEE Proc. Control Theory Appl., 2006, 153, (1), pp. 37–45

[5] Leyva R., Cid-Pastor A., Alonso C., Queinnec I., Tarbouriech S., Martinez-Salamero L.: 'Passivity-based integral control of a boost converter for large-signal stability', IEE Proc. Control Theory Appl., 2006, 153, (2), pp. 139–146

[6] Boyd S., EL Ghaoui L., Feron E., Balakrishnan V.: 'Linear matrix inequalities in system and control theory' (SIAM, 1994) Chapter 4

[7] Gahinet, P., Nemirovskin A., Laub A.J., Chilali M.: 'LMI control toolbox for use with matlab' (The MathWorks, Inc., 1995) Chapter 2

[8] Olalla, C.; Leyva, R.; El Aroudi, A.; Queinnec, I.; "Robust LQR Control for PWM Converters: An LMI Approach," *Industrial Electronics, IEEE Transactions on* , vol.56, no.7, pp.2548-2558, July 2009

[9] Olalla, C.; Leyva, R.; El Aroudi, A.; Garces, P.; Queinnec, I.; , "LMI robust control design for boost PWM converters," *Power Electronics, IET* , vol.3, no.1, pp.75-85, January 2010

[10] Gahinet, P., & Apkarian, P. (1994). A linear matrix inequality approach to H∞ control. *International Journal of Robust and Nonlinear Control*, *4*(4), 421-448.

[11] Chilali, M.; Gahinet, P. , "H∞ design with pole placement constraints: an LMI approach," Automatic Control, IEEE Transactions on , vol.41, no.3, pp.358-367, Mar 1996